Superspreading performance of branched ionic trimethylsilyl surfactant $Mg(AOTSiC)_2$

Kovalchuk, Nina M.; Sagisaka, Masanobu; Osaki, Suzuna; Simmons, Mark J.H.

DOI:
10.1016/j.colsurfa.2020.125277

Document Version
Publisher's PDF, also known as Version of record

Citation for published version (Harvard):
Kovalchuk, NM, Sagisaka, M, Osaki, S & Simmons, MJH 2020, 'Superspreading performance of branched ionic trimethylsilyl surfactant $Mg(AOTSiC)_2$', *Colloids and Surfaces A: Physicochemical and Engineering Aspects*, vol. 604, 125277. https://doi.org/10.1016/j.colsurfa.2020.125277

Colloids and Surfaces A 604 (2020) 125277

Contents lists available at ScienceDirect

Colloids and Surfaces A

journal homepage: www.elsevier.com/locate/colsurfa

Superspreading performance of branched ionic trimethylsilyl surfactant Mg(AOTSiC)$_2$

Nina M. Kovalchuk[a,*], Masanobu Sagisaka[b], Suzuna Osaki[b], Mark J.H. Simmons[a]

[a] School of Chemical Engineering, University of Birmingham, B152TT, UK
[b] Graduate School of Science and Technology, Hirosaki University, 036-8561, Japan

GRAPHICAL ABSTRACT

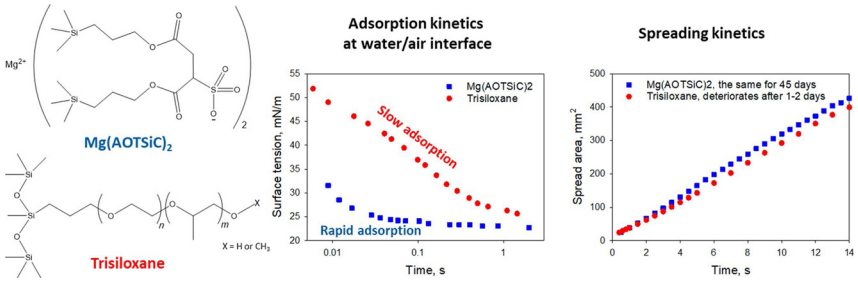

ARTICLE INFO

Keywords:
Aqueous surfactant solutions
Solid substrate
Complete wetting
Superspreading
Spreading kinetics
Dynamic surface tension

ABSTRACT

The spreading performance of aqueous solutions containing a novel branched trimethylsilyl hedgehog ionic surfactant, Mg(AOTSiC)$_2$, was compared with that of trisiloxane superspreaders on a hydrophobic polyvinylidenefluoride substrate. The work shows that Mg(AOTSiC)$_2$ is a superspreader with spreading kinetics similar to trisiloxane surfactants, demonstrating that a hammer-like molecular architecture is not a necessary requirement for superspreading. The aqueous solutions of Mg(AOTSiC)$_2$ are much more stable than trisiloxane solutions and retain the same spreading performance for at least 45 days. Comparison of the spreading kinetics with dynamic surface tension revealed that Mg(AOTSiC)$_2$ requires a 10 fold faster equilibration rate at the air/water interface to demonstrate the same spreading kinetics as trisiloxane superspreaders. Addition of 20 % glycerol to the Mg(AOTSiC)$_2$ solutions suppressed superspreading by slowing down surfactant diffusion; then only surfactant enhanced spreading with a time dependence of spread area $S \sim t^{0.8}$ was observed.

1. Introduction

The spreading of liquids over solid surfaces is an ubiquitous component of many natural phenomena, for example the wetting of soil by rain and of industrial processes including painting, printing, enhanced oil recovery, foliar application of pesticides and fertilisers in agriculture. In many applications, it is important to know not only whether the liquid wets the solid or not, but also how fast it spreads, especially in the case of complete wetting. If the liquid is not volatile, then the spreading time is theoretically unlimited and thus the equilibrium thickness of spreading film will be reached eventually. If the liquid is volatile and if the spreading is slow, liquid will evaporate before covering a noticeable area of the substrate, thus the maximum spread area is limited by the evaporation rate [1]. Therefore, understanding of the spreading kinetics is essential for volatile liquids including water.

Theoretical consideration of the spreading problem shows that at

* Corresponding author.
E-mail address: n.kovalchuk@bham.ac.uk (N.M. Kovalchuk).

https://doi.org/10.1016/j.colsurfa.2020.125277
Received 18 May 2020; Received in revised form 5 June 2020; Accepted 6 July 2020
Available online 10 July 2020

the very beginning, spreading is governed by inertia. However, the characteristic time scale of inertial spreading is very short, being smaller than 10 ms for mm-sized drops of water [2,3]. For later times, the spreading is viscosity mediated and in this viscous regime, the spread area of pure liquids increases with time according to Tanner's law $S \sim t^{0.2}$ [4,5], where S is the spread area and t is time. If a small mm-size water drop spreads on a hydrophilic substrate under normal ambient conditions, spreading is completely suppressed by evaporation on a time scale of tens of seconds [6,7]. In this case, the maximum spread area does not exceed several mm^2.

It should be stressed that pure water wets completely only highly hydrophilic substrates, such as clean glass or mica. Only partial wetting is possible on any polymeric surface, plant leaves or human skin. Surfactants are thus widely used to improve the wetting properties of aqueous formulations. For example, drops of pure water may only contact the tips of wax crystalloids and will eventually roll-out of many plant leaves. Therefore surfactants (activator adjuvants) are used in aqueous fertiliser and pesticide formulations to guarantee their effectiveness [8,9]. Thus, the effects of surfactants on the spreading kinetics of aqueous formulations are of great importance.

The derivation of Tanner's law was carried out under the assumption of constant surface tension. However, if a surfactant is present in a spreading drop, it can redistribute under the influence of the local flow field and due to adsorption on the newly created liquid/air and solid/liquid interface. Temporal and spatial variations in the local concentration of surfactant over the surface of spreading drop will cause surface tension gradients (and consequently Marangoni flows) which will change the value of spreading exponent. This can strongly influence the spreading kinetics and numerous experimental studies show that when a surfactant is added to an aqueous formulation, kinetics become much faster than for pure liquids. In many cases, the spread area increases proportionally to time or even faster and the maximum spread area for a mm size drop is of $O(10^2)$ larger than for pure water. This fast surfactant enhanced spreading is called superspreading and has been intensively investigated over the last few decades. There are numerous review papers regularly updating achievements in the area [10–16].

The essential characteristic features of superspreading include dependence of the spreading rate on substrate properties and surfactant concentration, see [11,17] and references herein. The spreading rate reaches a maximum on substrates partially wetted by pure water with a contact angle of $\sim 70^\circ$ and decreases rather quickly with an increase or a decrease of substrate hydrophobicity. There is also a certain optimal surfactant concentration at which the spreading rate/spread area has a maximum. The superspreading performance of trisiloxane surfactants depends also on ambient humidity [18,19] raising a question about the role of a precursor aqueous film in this phenomenon, ionic strength [19] and solution pH [20]. It should be noted that aqueous solutions of trisiloxane superspreaders are prone to hydrolysis resulting in a deterioration of their spreading properties [21].

Despite intensive studies, the precise mechanism of superspreading is not yet established. Considering that the best known superspreaders, trisiloxane surfactants, have an unusual hammer-like shape with bulky hydrophobic part and long hydrophilic tail, it has been suggested that the surfactant architecture is crucial for superspreading [22]. Such a shape is favourable for promoting a caterpillar-like motion of the propagating three phase contact line (TPCL) enabling direct transfer of surfactant from the liquid/air to the solid/liquid interface. According to [23] the caterpillar motion considerably reduces viscous dissipation in the vicinity of TPCL and therefore can accelerate spreading. Shape of TPCL characteristic for caterpillar motion was found in a molecular dynamics simulation on superspreading [24]. According to CFD simulations which have, for the first time, taken into account various mechanisms of transfer and adsorption of soluble surfactants during spreading [25], direct transfer of surfactant from the liquid/air to the solid/liquid interface through the TPCL results in a considerable acceleration of spreading kinetics. The favourability of a hammer-like shape for direct adsorption of surfactant molecules into the TPCL, leading to faster spreading, was also supported by results of molecular dynamics simulation [26], however according to [26], contribution of surfactant chemistry is more important.

The importance of surfactant adsorption in the vicinity of TPCL as well as a strong interaction of the surfactant with the solid substrate were both postulated as being important to the mechanism of superspreading. According to [27,28], surfactant molecules with high affinity for the solid surface adsorb sufficiently strongly to partially propagate beyond the TPCL to the solid/air interface. As in this case the hydrophilic part of the molecule is exposed to air, a surfactant bilayer should be formed at the solid/air interface to minimise the free energy. Bilayer formation was also observed in molecular dynamics simulations [26,29]. According to [28] the bulk water is sucked into the hydrophilic interior of the bilayer splitting it via an "unzipping" mechanism which propagates the spreading front. It is suggested in [27,28] that the above mechanism is facilitated by Marangoni flow directed towards the TPCL and caused by surfactant depletion in that region.

The Marangoni flows mentioned above have been identified in many studies as making an important contribution to the superspreading mechanism. As a drop spreads, surfactant in the vicinity of the TPCL is adsorbed onto the newly created liquid/air and solid/liquid interfaces. Therefore depletion of surfactant in this region is expected resulting in higher surface tension, whereas the surface tension in the central part of drop may remain unchanged. Therefore, under the action of surface tension gradient, liquid will flow in the direction of the TPCL (Marangoni flow) and contribute to the spreading kinetics. Obviously, the surface tension gradient depends on the surfactant concentration, diffusion coefficient and adsorption characteristics. Estimations performed in [30,31] have shown that, depending on the length scale on which the surface tension gradient is established, the spreading exponent can vary between 0.5 and 2 in good agreement with experimental data.

The role of Marangoni flows in superspreading is supported by both numerical simulations [25,32] and experimental studies [30,33,34]. Numerical studies in [25] show that spreading accelerates in the presence of a surfactant as a result of surfactant depletion at the liquid/air interface and formation of strong gradients of surface tension in the vicinity of the TPCL. The essential parameters affecting spreading performance are the surfactant concentration, the kinetics of surfactant adsorption on liquid/air and solid/liquid interfaces, the limiting adsorption on solid/liquid interface and the possibility of direct adsorption of surfactant from liquid/air to solid/liquid interface through the TPCL [25].

A mechanism based on Marangoni flow can explain the known regularities of superspreading [12,30]. For example, a maximum in the spreading rate dependence on surfactant concentration can be explained as follows. The spreading rate due to the Marangoni flow is proportional to the surfactant concentration gradient. Assuming that the characteristic length over which the concentration gradient is formed remains constant, the maximum gradient appears when the surface tension near the drop centre is close to the equilibrium value, whereas that in the vicinity of the TPCL is equal to pure water. If the surfactant concentration is too small, then the equilibration rate is too slow, so the surface tension in the centre of spreading drop can be larger than the equilibrium value and therefore the surface tension gradient does not reach its maximum. Conversely, if the concentration is too high, the surfactant equilibrates too rapidly resulting in lower surface tension near the TPCL, i.e. again smaller than the maximum surface tension gradient. Thus if the equilibration rate slows down (for example due to a decrease in the diffusion coefficient) then the concentration corresponding to the maximum spreading rate has to increase. Such a dependence of optimum concentration on diffusion coefficient has been confirmed experimentally in [34].

The contribution of Marangoni flow to the superspreading

mechanism is now broadly accepted, but many questions remain unanswered. Are there other contributions and what are they? Is the surfactant architecture crucial for superspreading? How exactly are the gradients of surface tensions formed? What is the role of adsorption on solid/liquid interface and the possibility of direct surfactant transfer through TPCL? The importance of adsorption on the solid/liquid interface, for example, is confirmed by the fact that aqueous solutions of fluorosurfactants, which have lower surface tension than trisiloxane solutions, usually do not have superspreading properties [35].

As highlighted above, experimental studies of superspreading have focused mostly on trisiloxane surfactants and a broader range of superspreaders is required, with various architectures and adsorption characteristics, to tackle the above questions. However, literature on new superspreaders is rather scarce. Synthesis of double-tailed trisiloxane surfactants with improved resistance to hydrolysis was reported in [36], but the spreading of these surfactants was studied on parafilm, where only partial wetting took place. Synthesis of gemini-type trisiloxane surfactants and their spreading performance on rice and mango leaves was studied in [37], reporting superspreading behaviour for some of them. The fluorinated surfactant, perfluoropolyether amide propyl betaine, was found to completely wet parafilm as reported in [38], however the spreading kinetics were not studied in [38] and therefore it is not known whether this surfactant is a superspreader.

To fill this gap, the spreading performance of a new surfactant, the magnesium salt of bis (3-(trimethylsilyl)-propyl) 2-sulfosuccinate, Mg $(AOTSiC)_2$, is presented below. The main distinctive features of Mg $(AOTSiC)_2$ are that

i) it is an ionic surfactant and has considerably higher critical aggregation concentration (CAC) than non-ionic trisiloxane superspreaders;
ii) it is a branched trimethylsilyl hedgehog surfactant with a brush-like structure [39], see Fig. 1, thus its architecture is different from that of T-shaped trisiloxane surfactants;
iii) trisiloxane surfactants contain a –O-Si-O-Si- backbone making them prone to hydrolysis, whereas in $Mg(AOTSiC)_2$ the silicon atom is connected only to carbon atoms (see Fig. 1) therefore it is expected to be much more stable in aqueous solutions [39].

In this paper, the spreading kinetics of $Mg(AOTSiC)_2$ in the regime of complete wetting are studied over a range of concentrations and compared with a trisiloxane superspreader using a similar substrate. The other experimental parameters, such as drop volume, ambient temperature and humidity are chosen to match experimental conditions used in experiments with trisiloxane surfactants. Special attention is paid to comparison of the spreading performance with surfactant equilibration rate at the liquid/air interface assessed through the dynamic surface tension.

Kinetics of surfactant transfer is one of the critical parameters in superspreading. The rate of diffusion transfer is proportional to both surfactant diffusion coefficient and concentration gradient, i.e. surfactant equilibrates faster in more concentrated solutions. To separate the contribution of concentration and diffusion coefficient on the transfer rate, a set of experiments was performed using surfactant solutions in 20 % glycerol/80 % water mixture. The glycerol/water mixture has viscosity 1.8 mPa·s, i.e. nearly twice larger than water viscosity. Whilst such an increase in viscosity has a negligible effect on the spreading kinetics in the case of pure liquids [34], it results in a diffusion coefficient of surfactant which is approximately half that for pure water.

2. Experimental

$Mg(AOTSiC)_2$ (molecular mass M = 875.66 g/mol) was synthesised according to the procedure presented schematically in Fig. 1. A detailed description of this synthetic procedure is given in the supplementary information S1.

$Mg(AOTSiC)_2$ belongs to a novel class of branched trimethylsilyl hedgehog surfactants [39]. These surfactants have a brush-like structure enabling a tight packing of hydrophobic tails at a water/air or water/oil interface with mostly methyl groups connected to silicon being exposed. Such a combination has the lowest energy among hydrocarbon tails. Therefore, solutions of these surfactants demonstrate a very low surface/interfacial tension. The surface tension isotherm presented in Fig. 2 demonstrates that the surface tension of Mg $(AOTSiC)_2$ at concentrations above critical aggregation concentration (CAC = 0.47 mM = 0.412 g/L) is σ = 21.8 mN/m, which is close to the surface tension of trisiloxane superspreaders [34]. Here the term CAC is used instead of critical micelle concentration, CMC, to include any self-assembled structures formed in solution, not just micelles. Fitting the results of Fig. 2 for concentrations below CAC with the Szyszkowski–Langmuir equation of state

$$\sigma_0 - \sigma = nRT\Gamma_\infty \ln(1 + bc) \quad (1)$$

under the assumption that bc > > 1, gives the parameters of Langmuir adsorption isotherm for this surfactant as $\Gamma_\infty = 1.2{\cdot}10^{-6}$ mol/m^2 and $b = 6.4{\cdot}10^2$ m^3/mol. In Eq. (1) σ_0 is the surface tension of pure water at absolute temperature T = 298 K, R is the gas constant, Γ_∞ is the limiting adsorption, b is a parameter reflecting the surface activity of the surfactant and n accounts for the number of ions in the dissociated molecule. The value n = 3 was used for the fitting procedure. Therefore the limiting adsorption here was calculated for the surfactant molecule as a whole [40]. The area per molecule at the CAC for $Mg(AOTSiC)_2$ is 142 A^2, much larger than for trisiloxane surfactants whose values range from 53 – 66 A^2 [12,41].

The surfactant was dissolved at a maximum concentration of 60 times the CAC in water and 20 CAC in 20 wt % glycerol mixture with water. Dissolution was carried out using a roller mixer over 48 h with a periodic application of vibration. Afterwards, the solutions were sonicated for 10 h and left on the roller mixer for another 14 h. Then, the solutions were diluted to concentrations of 2, 4 and 8 CAC. Additionally, solutions of 16 and 30 CAC were prepared in water. Note that a solution with a concentration of 1 CAC was prepared, but discarded because it does not demonstrate complete wetting of the substrate used in this study. Double-distilled water was produced by an Aquatron A 4000 D water still (Stuart). Glycerol (Alfa Aesar, ultrapure, HPLC grade) was used as received. The glycerol/water mixture used in this study has a density of 1049 kg/m^3 and a viscosity of 1.8 mPa·s [42].

Polyvinylidenefluoride (PVDF) film (GoodFellow) with a thickness of 0.05 mm was used as a substrate. The substrate has a noticeable roughness with parallel grooves, $R_{rms} \sim 0.5$ µm [33]. The contact angle of water on this substrate was 81 ± 3°, measured using a Profile Analysis Tensiometer PAT-1 P (Sinterface) in sessile drop mode. The large error in contact angle determination is due to the rather opaque surface of the samples which did not give a good reflection of the drop; therefore there was uncertainty in identifying the contact line between the drop and substrate surface in the image.

To take into account any possible non-uniformity in chemical composition and structure (roughness) of the substrate, 6 pieces of size ~ 40 × 40 mm were cut from the original film, numbered and used throughout the whole study. On each substrate sample, spreading experiments were carried out at least 3 times, for some 4 or 5 times, to estimate the ageing properties of surfactant solutions. Glass microscope slides (Corning Incorporated) were used as a support for the films. Before each spreading experiment, substrates were washed with ethanol absolute (Fisher), rinsed with plenty of double-distilled water, dried on a hotplate at 35 °C for 20–25 min and conditioned at room temperature for 5 min.

A drop of surfactant solution with a volume of 5 mm^3 was deposited immediately on the substrate using an Eppendorf pipette. Spreading was recorded using a Photron SA3 camera equipped with a AF NIKON 24–85 mm lens at 60 fps with an exposure time of 0.5 ms and a spatial resolution of 40 µm/pixel. The time zero for the measurement

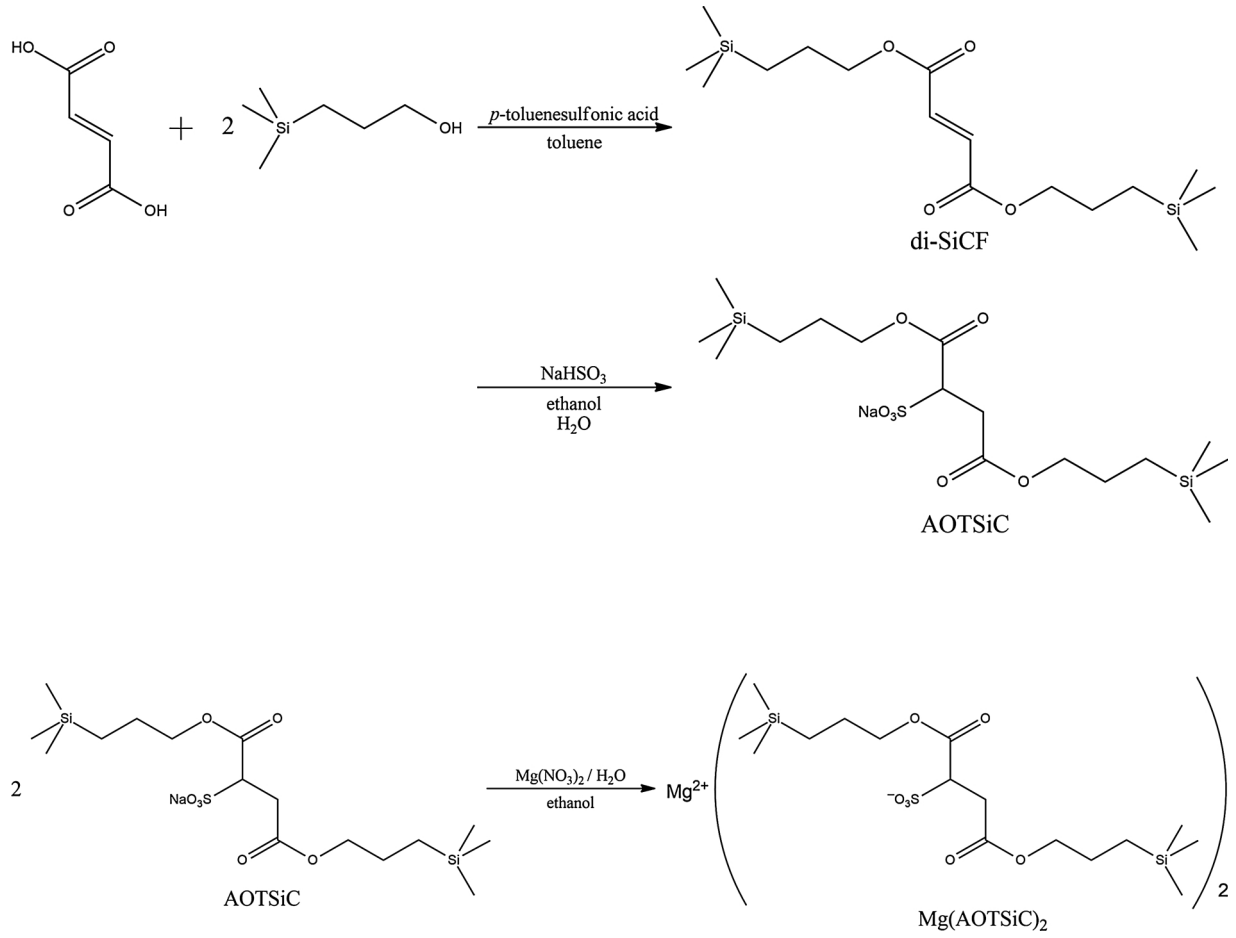

Fig. 1. Pathway for synthesis of the anionic surfactant $Mg(AOTSiC)_2$.

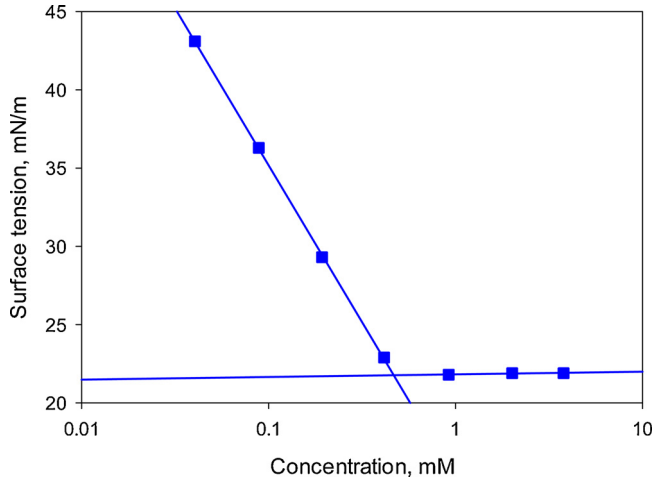

Fig. 2. Surface tension isotherm of $Mg(AOTSiC)_2$ at ambient temperature T = 25 °C.

corresponded to the moment when the drop touched the substrate. All measurements were performed at a temperature, T = 23 ± 1 °C and a relative humidity, RH = 44 ± 2 % as measured by a temperature/humidity meter (Fisher).

Image processing was carried out by ImageJ free software [43]. The spread area after 6 s and 14 s of spreading (see Results and Discussion for the choice of characteristic spreading time) was measured for all samples and all runs. Afterwards, the average spread area for each concentration was calculated. The spreading kinetics for each concentration was studied for one selected run (including all 6 substrate samples) plus for one or two selected substrates (including all available runs for these substrates). The selection criterion for the chosen run/substrate was the one which possessed an average area after 14 s closest to the average value calculated over all runs and substrates. Therefore, spreading kinetics was studied for at least 8 cases at each concentration.

Dynamic surface tension was measured by a maximum bubble pressure tensiometer BPA-1S (Sinterface) and equilibrium surface tension was measured with a pendant-drop tensiometer made in-house using a gauge 28 needle (o.d. 0.362 mm and i.d. 0.184 mm) [44].

3. Results and discussion

3.1. Properties of surfactant solutions

After preparation, all solutions exhibited a turbidity which increased with concentration. When solutions were left unmixed for a long time, a precipitate was slowly formed at the bottom. The precipitate was formed not only at room temperature, but also at higher temperatures, up to 70 °C. The obvious assumption is that the Kraft temperature for this surfactant is above 70 °C and that all concentrations used in this study exceeded the solubility limit, i.e. the precipitate was composed of undissolved macroscopic particles. In this case, it could be expected that the spreading performance of the surfactant solutions is independent of concentration. However, as shown below, an increase in the surfactant concentration results in an improved spreading performance. Moreover, although the equilibrium surface tension at concentrations above the CAC is practically independent of concentration, the dynamic surface tension depends on concentration, with faster equilibration at larger concentrations as shown in Fig. 3.

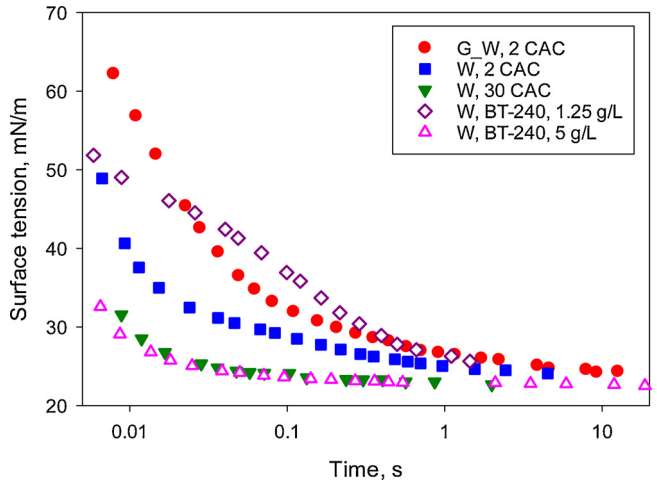

Fig. 3. Dynamic surface tension of $Mg(AOTSiC)_2$ solutions in water, W and water/glycerol mixture, G_W (filled symbols) compared to dynamic surface tension of trisiloxane superspreader BT-240 in water having the same equilibrium surface tension [34] (empty symbols).

Therefore, it can be assumed that the precipitate, at least to some extent, is formed by self-assembled structures which can rapidly replenish and thus maintain the bulk concentration as surfactant is lost to adsorption on the newly created interface.

Notably, the time dependence of the dynamic surface tension of original mixed samples does not change considerably after filtration through a 450 nm or even a 200 nm syringe filter, i.e. the main contribution to the dynamic surface tension is provided by self-assembled structures with a size below 200 nm, most probably due to their higher mobility. The equilibration of solutions prepared in the water/glycerol mixture is considerably slower than for the purely aqueous solutions (Fig. 3). This is the result of smaller diffusion coefficient caused by larger viscosity. For comparison, data on the dynamic surface tension of the superspreading trisiloxane surfactant BT-240 (Evonic) from Ref [34] are also included in Fig. 3. Note, the CAC value for BT-240 is around 0.06 g/L.

The prepared samples were kept for more than one month with periodic sonication and further mixing on the roller mixer. No significant change in the spreading performance was observed when compared with the fresh samples. Therefore, it can be concluded that there was an equilibrium between the surfactant in solution and the precipitate. This supports an assumption that the precipitate is formed by self-assembled structures, which are supposed to be in thermodynamic equilibrium with monomers in the bulk liquid. It can be also concluded that the spreading performance of $Mg(AOTSiC)_2$ does not deteriorate with time, including for the filtered solutions. This is a significant advantage when compared with traditional trisiloxane superspreaders whose spreading performance quickly declines with time due to hydrolysis [21].

3.2. Spreading performance of $Mg(AOTSiC)_2$ solutions in water

A typical spreading process is presented in Fig. 4. After the drop touches the substrate, there is always some transition period related to the inertia of the drop during deposition following detachment from the pipette tip, after which quasi-stationary spreading was observed. To exclude those disturbances as well as relatively large measurement errors for small areas, the spread area used for kinetics analysis was taken for $t \geq 0.5$ s. During the first 1 − 2 s the spreading front was practically circular (the very inner ring in Fig. 4). However, at t = 3 s, the shape changed and became elongated in the direction of the grooves on the substrate. The movement perpendicular to the grooves is retarded because the real surface area in this direction is considerably larger than

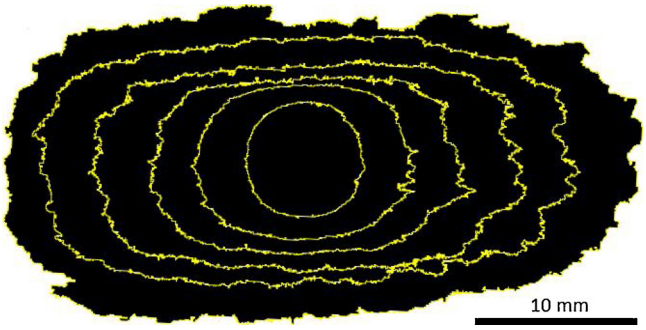

Fig. 4. Binary images of spread area vs time for 5 mm^3 drop of 30 CAC solution in water filtered through 200 nm syringe filter. The contours correspond to the spreading time 1, 3, 5, 8, 12 and 20 s.

the projected area. The movement in the direction of the grooves can be further accelerated due to effect of capillary wicking [45]. The change of the spreading shape from circular to elongated can be a manifestation of a change in the spreading mechanism.

At maximum spreading, the thickness of the film was less than 10 μm. As the spreading proceeds and the area covered by the surfactant solution increases, the optical contrast between the wetted and unwetted substrate decreases. Therefore, the reliable calculation of the spread area becomes problematic, if not impossible. In addition, at large spread areas and on sufficiently large time scales, the spreading kinetics can be affected by evaporation [1,6,7]. Thus, to mitigate these issues, the spreading kinetics of solutions in water was studied at $t \leq 15$ s. Longer time scales ($\geq$ 20 s) were considered for the glycerol/water solutions due to their slower spreading and considerably slower evaporation.

The spreading performance was dependent upon the substrate used, with the lowest spread area consistently shown on substrate S4, whereas the highest spread area was shown on substrate S1. The difference in spread area between the substrates at t = 14 s was normally within 30 %, but for the case of high concentration, 60 CAC, filtered through the 450 nm coarse filter it was around 50 % as shown in Fig. 5. The legend of Fig. 5 shows relative humidity, RH, for each measurement. This parameter remained practically the same, as was the temperature, T, because measurements presented in Fig. 5 were performed within several hours.

Another example of spreading kinetics is given in Fig. 6, where the results for several runs on the same substrate are presented. The figure shows that the variations of the temperature and humidity within the range used in this study have no noticeable effect on spreading. All

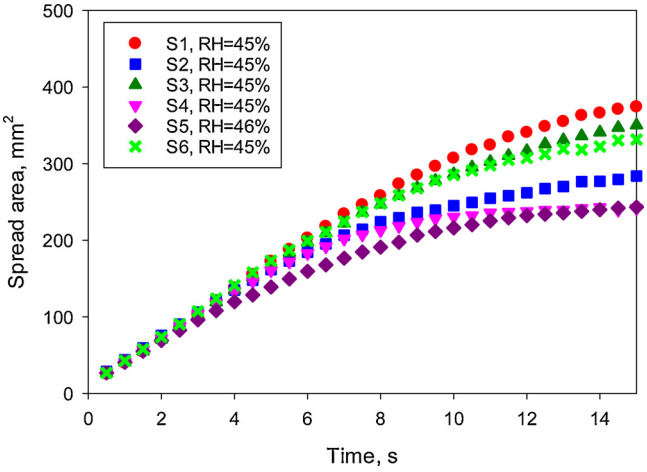

Fig. 5. Spreading kinetics of 60 CAC solution of $Mg(AOTSiC)_2$ in water filtered through 450 nm filter, Run 2 on various substrates at temperature T = 23 °C.

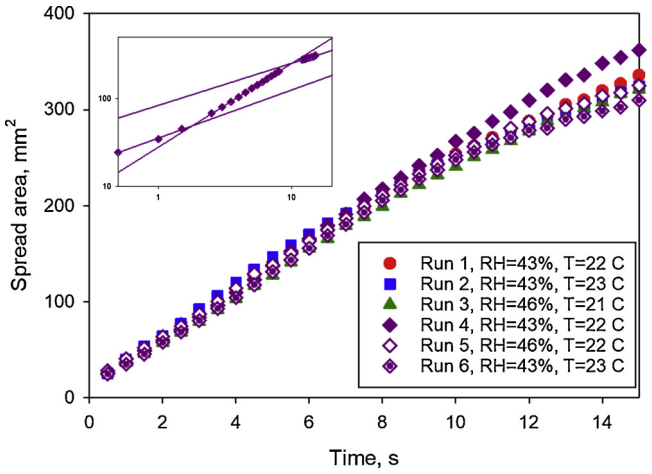

Fig. 6. Spreading kinetics of 8 CAC solution of $Mg(AOTSiC)_2$ in water on substrate S4.

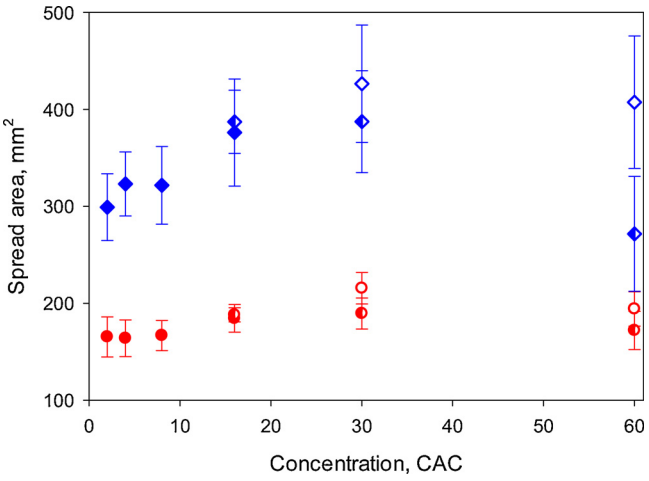

Fig. 7. Dependence of spread area on surfactant concentration: circles at t = 6 s, diamonds at t = 14 s; filled symbols – not filtered solutions, half-filled symbols – solution filtered through 450 nm syringe filter, empty symbols – solutions filtered through 200 nm syringe filter.

these measurements were performed on the same substrate, but on different days. Runs 4–6 were performed on the same day, 45 days later than Run 1. Thus, Fig. 6 clearly shows that the spreading performance of solution is unaffected by time, at least within 45 days. The sample for the Run 6 was sonicated for 15 min immediately before the spreading experiment, whereas the other samples were premixed for 15 min on a roller mixer. Clearly, the sonication at this stage has no noticeable effect on the spreading performance.

Figs. 5 and 6 show that spreading slows down with time and that this slowing down depends on solution concentration. The inset in Fig. 6 shows data for Run 6 on a logarithmic scale, demonstrating that there are three distinct spreading regimes, each following a power law relationship with a different exponent. On the shortest time scale, first stage, $t \leq 2$ s, when the spreading profile is circular (Fig. 4), spreading is rather slow. It considerably accelerates later in the second stage and then slows down again in the third stage. These three stages of spreading are in good agreement with results for trisiloxane superspreaders [34]. The duration of the second stage depends on surfactant concentration (compare Fig. 5 and 6) and varies slightly between substrates, but in most cases spreading slows down for $t > 10$ s. Thus, the spreading exponent for the second stage was calculated between $2\text{ s} < t < 8\text{ s}$ and that for the third stage between $11\text{ s} < t < 15\text{ s}$. As well as the spreading exponents, the average spread area (over all runs and substrates) was used to characterise the spreading performance. Two different time points were chosen to calculate the representative spread areas: t = 6 s within the second stage and t = 14 s within the third stage. The last time value is also chosen for convenience of comparison with results for trisiloxane superspreaders, which are reported in [34] for t = 14 s.

Run 4 in Fig. 6 demonstrates faster spreading than the other runs. The difference reveals itself at $t > 9$ s, and could be due to a variation in the substrate drying conditions and larger residual water content on substrate in Run 4. This assumption is supported by the fact that the spread area at 14 s was on average 13 % higher for the substrates dried at room temperature when compared with substrates dried at 35 °C. However, the study of the effect of drying conditions was limited here to one concentration, 30 CAC, and only for one run over the whole set of substrates. Therefore, a more thorough study on the subject is required, employing a humidity chamber, where the substrates can be conditioned within a range of precisely controlled humidity values.

To study the effect of the sediment presented, a comparison was performed between the non- filtered samples and those filtered through 200 nm and 450 nm syringe filters. There was no difference at small surfactant concentrations. A noticeable, although small, difference between unfiltered and filtered samples appeared at a concentration of 16 CAC, whereas at 30 CAC, differences between the 200 nm and 450 nm filtered samples could be discriminated, as shown in Fig. S2. In all cases, removal of large particles resulted in a better spreading performance. Note, the spreading kinetics of trisiloxane surfactant BT-240 [34] is shown in Fig. S2 for comparison.

The dependence of spread area on surfactant concentration is presented in Fig. 7. At both t = 6 and 14 s there is a distinctive maximum versus concentration corresponding to 30 CAC. Note, the relatively large experimental errors in Fig. 7 are mainly due to the difference between substrates, however the results for each substrate had smaller experimental errors and were consistent with the dependencies presented in Fig. 7. The optimal concentration value is higher than that for trisiloxane surfactants, where the maximum in spread area was observed at concentrations in the range 10–20 CAC. It should be stressed that CAC for $Mg(AOTSiC)_2$ is 5–10 times higher than that for trisiloxane surfactants, i.e. the difference in the molar concentration is even higher. Comparison with data for trisiloxane superspreaders on the same substrate [34] shows that the maximum spread area at t = 14 s is very similar, around 400 mm^2, for the same drop volume of 5 mm^3 (a value more than 100 times larger than for the pure liquid on the same timescale).

Comparison of the surfactant dynamic surface tension for $Mg(AOTSiC)_2$ and trisiloxane surfactant BT-240 (Fig. 3) shows that the dynamic surface tension for 30 CAC of $Mg(AOTSiC)_2$ on a time scale of 5 ms – 20 s is similar to that of BT-240, at 5 g/L. This concentration of BT-240 is much higher than the optimum concentration of 1.25 g/L and spreading of corresponding solution slows down with transition to the third stage at $t \sim 6$ s. The spread area at 14 s for solution of BT-240, 5 g/L is only around 200 mm^2. On the other hand, the dynamic surface tension for the optimal concentration of BT-240, 1.25 g/L is even higher that for $Mg(AOTSiC)_2$ at 2 CAC. The last concentration is too small for $Mg(AOTSiC)_2$ and provides a spread area of around only 300 mm^2, considerably below the maximum spread area.

In [34], the diffusion coefficient of surfactant was varied by changing the viscosity of the aqueous phase through addition up to 40 % of glycerol. It was shown that similar changes in the viscosity of pure liquids do not affect the spreading kinetics and therefore all changes in spreading performance of surfactant solutions in the presence of glycerol were related to the changes in surfactant equilibration rate. An increase in solution viscosity and therefore a decrease in surfactant diffusion coefficient shifted the maximum in spread area to larger concentrations. Dynamic surface tension corresponding to the optimum concentration also changed: faster equilibration was observed for a

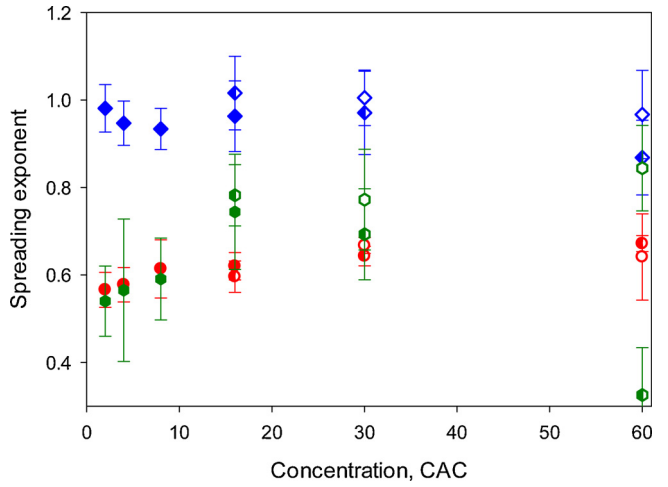

Fig. 8. Dependence of spreading exponents on surfactant concentration: circles – stage 1, diamonds – stage 2, hexagons – stage 3; filled symbols – not filtered solutions, half-filled symbols – solution filtered through 450 nm syringe filter, empty symbols – solutions filtered through 200 nm syringe filter.

larger optimum concentration, however the difference was not very large. Notably, the best spreading performance, independent of glycerol concentration, was observed for solutions reaching equilibrium surface tension on a time scale of 1 s. For $Mg(AOTSiC)_2$, the best spreading performance was observed at an equilibration time of 0.1 s: it seems that for a surfactant with 10 times larger CAC, equilibration should be 10 times faster to provide the best performance. Thus, comparing the results of [34] and the present work it can be concluded that essential changes in the type of surfactant, namely in its architecture, activity and CAC value, result in considerable changes in the required surfactant equilibration rate on the liquid/air interface. This highlights the crucial role of surfactant adsorption on the solid/liquid interface and the conditions for direct adsorption from liquid/air to solid/liquid interface through the TPCL [25].

Fig. 8 presents the concentration dependent spreading exponent for each stage. The spreading exponent for the first stage is around $\alpha_1 = 0.6$ and slightly increases with concentration. This value is slightly larger than found for trisiloxane solutions in water (α_1 in the range $0.3-0.5$) [34], and the duration of the first stage is also larger (< 1 s for trisiloxanes). Note, addition of glycerol in [34] increased considerably the duration of stage 1, but also increased the spreading exponent in this stage. Such a correlation is in line with the results for $Mg(AOTSiC)_2$ obtained here. Thus, it can be speculated that for superspreading to begin a certain surfactant distribution (probably surfactant concentration gradients) should be achieved and this is what happens during the first stage.

The spreading exponent in the second stage was around $\alpha_2 = 1$ (similar to trisiloxane superspreaders) for all studied solutions except for 30 CAC solution filtered through 450 nm filter, i.e. $Mg(AOTSiC)_2$ is a superspreader. Considering that the molecular architecture of $Mg(AOTSiC)_2$ is very different from trisiloxanes, it can be concluded that the hammer-like shape of trisiloxane molecules is not a necessary precondition for superspreading to occur. A decrease in the spreading exponent for the second stage with an increase of surfactant concentration was observed also for trisiloxane surfactants [34]. Comparison of the data in Figs. 5 and 6 shows, that for 60 CAC solution, transition to the third stage occurred earlier than for concentration of 8 CAC and the spreading in the third stage was slower, the last result is reflected also in Fig. 8. Overall, the results in Fig. 8 show clearly that the improvement of the spreading performance in the studied range of concentrations is mostly due to an increase of the spreading exponent in the third stage, alongside the larger duration of the second stage. This is in line with the results for trisiloxanes, where for the best performing surfactants, the third stage was not observed at all within the time span of observation.

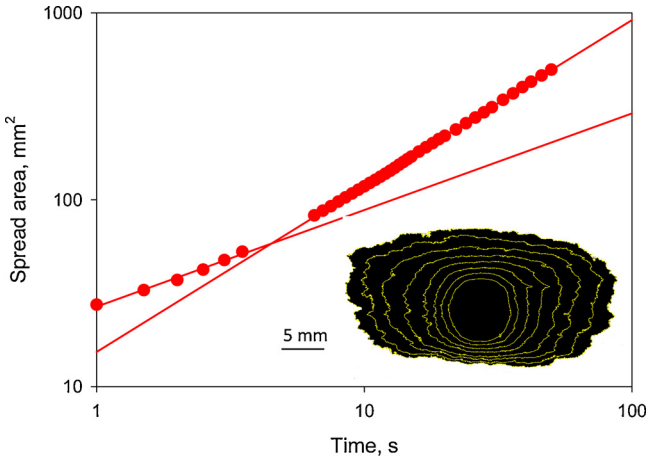

Fig. 9. Spreading kinetics of 20 CMC solution of $Mg(AOTSiC)_2$ in 20 % GL_W mixture. Inset shows the contours correspond to spreading time of 3 s, 5 s, 8 s, 12 s, 18 s, 26 s, 36 s and 46 s. Spread area at t = 50 s is 497 mm^2.

3.3. *Spreading performance of $Mg(AOTSiC)_2$ solutions in 20 % glycerol/80 % water mixtures*

The spread area for solutions in glycerol/water mixture on the time scale of observations is practically independent of concentration and for t = 14 s it is around 160 mm^2 (see Fig. S3), i.e. much smaller than that for solutions in water. The equilibration rate of solutions in G–W is considerably slower than those in water (Fig. 3), showing that the surfactant equilibration rate rather than the concentration is the parameter affecting the spreading behaviour. It should be however noted that, due to slower evaporation, the spreading of solutions in glycerol/water mixture lasts longer due to slower evaporation and as a result the maximum spread area achieved is comparable with that of water (see Fig. 9).

The kinetics of spreading of solutions in glycerol/water mixture is different from those in water. Only two stages were observed (Fig. 9) and spreading exponents for these stages are practically independent of surfactant concentration (Fig. 10). The first stage has a spreading exponent of $\alpha_1 \sim 0.54$, slightly lower than the exponent for solution of 2 CAC in water ($\alpha_1 = 0.57$), although this difference is in the range of experimental error. It lasts longer, up to 4 s, than the first stage for

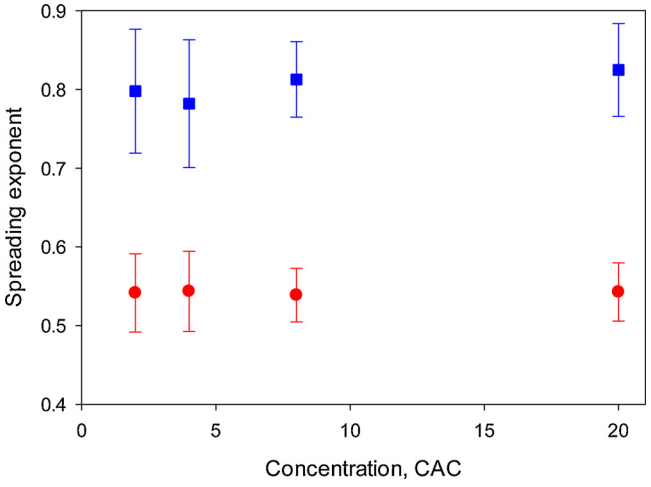

Fig. 10. Dependence of spreading exponents on surfactant concentration for solutions in glycerol/water mixture: circles – stage 1, squares – stage 2.

solutions in water. This is in line with assumption that the first stage provides some initial surfactant distribution necessary for the faster spreading to begin.

Spreading exponent for the second stage is around $\alpha_1 = 0.8$, similar to the highest exponent observed for solutions in water in the third stage, i.e. technically solutions in glycerol/water mixture do not superspread, as superspreading is related to the spreading exponent of 1 and higher. This shows that most probably there are at least two mechanisms contributing to a fast spreading of surfactant solutions: one is superspreading itself and another is surfactant enhanced spreading, which is slower, but still faster than the spreading of pure liquids [11]. This corresponds to the spreading of solutions in glycerol/water mixture and the third stage of spreading of solutions in water.

4. Conclusions

A study of the spreading performance of aqueous solutions of magnesium salt of bis (3-(trimethylsilyl)-propyl) 2-sulfosuccinate, Mg $(AOTSiC)_2$, a branched trimethylsilyl hedgehog surfactant with a brush-like structure and its comparison with the performance of trisiloxane superspreaders on the same substrate, polyvinylidenefluoride, has shown the following.

1 $Mg(AOTSiC)_2$ is a superspreader. It enables a very fast spreading kinetics for aqueous formulations with spread area being proportional to time. The spreading performance of $Mg(AOTSiC)_2$ is similar to the spreading performance of trisiloxane superspreaders on the same substrate. Notably, within 14 s of spreading, the area covered by both surfactant solutions increases more than 100 times and reaches 400 mm^2 for a drop of 5 mm^3 volume. This highlights that the specific hammer-like molecular architecture of trisiloxanes is not a necessary condition for superspreading.
2 The spreading performance of $Mg(AOTSiC)_2$ solution remains the same for at least 45 days. This is a considerable advantage in comparison with solutions of trisiloxane superspreaders, which are prone to hydrolysis and show a marked deterioration of spreading performance after $1-2$ days.
3 Similar to trisiloxane superspreaders, solutions of $Mg(AOTSiC)_2$ in water show a maximum in spread area vs concentration and three distinctive stages in spreading kinetics with different power law spreading exponents, α, for time dependence of spread area $S \sim t^{\alpha}$. The first stage lasts around 2 s and is characterised by the spreading exponent $\alpha_1 \sim 0.6$. Most probably it is related to the initial distribution of surfactant necessary for superspreading to begin. The second stage with $\alpha_2 \sim 1$ is the superspreading stage, which lasts 6–8 s. After that spreading slows down in the third stage of surfactant enhanced spreading with spreading exponent $\alpha_3 \leq 0.8$.
4 Comparison of dynamic surface tension corresponding to the optimum surfactant concentration shows that the best spreading performance of trisiloxane superspreaders was observed for solutions reaching equilibrium surface tension on the time scale of 1 s, whereas for $Mg(AOTSiC)_2$ the best spreading performance was observed at larger concentration, 30 CAC, and a much shorter equilibration time at air/liquid interface of 0.1 s. Thus the essential changes in the type of surfactant, namely in its architecture, activity and CAC value, result in considerable changes in required surfactant equilibration rate at liquid/air interface, displaying the importance of surfactants adsorption on solid/liquid interface for spreading performance of surfactant solutions.
5 Addition of 20 % of glycerol to $Mg(AOTSiC)_2$ solutions results in an approximately twofold decrease of the surfactant diffusion coefficient. For these solutions, superspreading was not observed in the range of surfactant concentrations between 2–20 CAC; instead two stages were identified. The first stage was similar to the first stage of solutions in water, but lasted longer, up to 4 s, whereas the second stage lasted up to 60 s and was characterised by the spreading exponent $\alpha_2 \sim 0.8$, close to the spreading exponent of the solutions in water during the third stage. This stage can be denoted as a surfactant enhanced spreading, which is more common phenomenon than superspreading.

CRediT authorship contribution statement

Nina M. Kovalchuk: Conceptualization, Methodology, Investigation, Visualization, Writing - original draft. **Masanobu Sagisaka:** Conceptualization, Methodology, Visualization, Resources, Funding acquisition, Writing - review & editing. **Suzuna Osaki:** Investigation. **Mark J.H. Simmons:** Conceptualization, Resources, Funding acquisition, Writing - review & editing.

Declaration of Competing Interest

The authors declare that there are no conflicts of interest.

Acknowledgments

Support from the Engineering & Physical Sciences Research Council, UK, through the PREMIERE Programme Grant EP/T000414/1 and from Japan Society for the Promotion of Science (KAKENHI, Grant-in-Aid for Scientific Research (B), No. 19H02504, Fostering Joint International Research (A), No. 15KK0221, Grant-in-Aid for Challenging Research (Exploratory), No.17K19002) is gratefully acknowledged.

Appendix A. Supplementary data

Supplementary material related to this article can be found, in the online version, at doi:https://doi.org/10.1016/j.colsurfa.2020.125277.

References

[1] S. Semenov, A. Trybala, R.G. Rubio, N. Kovalchuk, V. Starov, M.G. Velarde, Simultaneous spreading and evaporation: recent developments, Adv. Colloid Interface Sci. 206 (2014) 382–398.
[2] J.C. Bird, S. Mandre, H.A. Stone, Short-time dynamics of partial wetting, Phys. Rev. Lett. 100 (2008).
[3] X. Wang, L. Chen, E. Bonaccurso, J. Venzmer, Dynamic wetting of hydrophobic polymers by aqueous surfactant and superspreader solutions, Langmuir 29 (2013) 14855–14864.
[4] L. Tanner, The spreading of silicone oil drops on horisontal surfaces, J. Phys. D Appl. Phys. 12 (1979) 1473–1484.
[5] V.M. Starov, V.V. Kalinin, J.D. Chen, Spreading of liquid drops over dry surfaces, Adv. Colloid Interface Sci. 50 (1994) 187–221.
[6] R.D. Deegan, Pattern formation in drying drops, Phys. Rev. E 61 (2000) 475–485.
[7] C. Poulard, G. Guena, A.M. Cazabat, Diffusion-driven evaporation of sessile drops, J. Phys. Condens. Matter 17 (2005) 4213–4227.
[8] V. Fernández, T. Eichert, Uptake of hydrophilic solutes through plant leaves: current state of knowledge and perspectives of foliar fertilization, Crit. Rev. Plant Sci. 28 (2009) 36–68.
[9] V.J. Pereira, J.P.A.Rd. Cunha, T.Pd. Morais, J.P.Rd. Oliveira, J.Bd. Morais, Physical-chemical properties of pesticides: concepts, applications, and interactions with the environment, Biosci. J. 32 (2016) 627–641.
[10] R.M. Hill, Superspreading, Curr. Opin. Colloid Interface Sci. 3 (1998) 247–254.
[11] J. Venzmer, Superspreading — 20years of physicochemical research, Curr. Opin. Colloid Interface Sci. 16 (2011) 335–343.
[12] A. Nikolov, D. Wasan, Current opinion in superspreading mechanisms, Adv. Colloid Interface Sci. 222 (2015) 517–529.
[13] N.M. Kovalchuk, A. Trybala, O. Arjmandi-Tash, V. Starov, Surfactant-enhanced spreading: experimental achievements and possible mechanisms, Adv. Colloid Interface Sci. 233 (2016) 155–160.
[14] A. Sankaran, S.I. Karakashev, S. Sett, N. Grozev, A.L. Yarin, On the nature of the superspreaders, Adv. Colloid Interface Sci. 263 (2019) 1–18.
[15] P.E. Theodorakis, E.A. Müller, R.V. Craster, O.K. Matar, Insights into surfactant-assisted superspreading, Curr. Opin. Colloid Interface Sci. 19 (2014) 283–289.
[16] P.E. Theodorakis, E.R. Smith, R.V. Craster, E.A. Müller, O.K. Matar, Molecular dynamics simulation of the superspreading of surfactant-laden droplets. A review, Fluids 4 (2019).
[17] R.M. Hill, Superspreading, Curr. Opin. Colloid Interface Sci. 3 (1998) 247–254.
[18] S. Zhu, W.G. Miller, L.E. Scriven, H.T. Davis, Superspreading of water-silicone surfactant on hydrophobic surfaces, Colloids Surf. A Physicochem. Eng. Asp. 90 (1994) 63–78.
[19] J. Venzmer, S.P. Wilkowski, Trisiloxane surfactants – mechanism of spreading and

wetting, in: J.D. Nalewaja, G.R. Goss, R.S. Tann (Eds.), Pesticide Formulations and Application Systems, American Society for Testing and Materials, 1998, pp. 140–151.
[20] J. Radulovic, K. Sefiane, M.E. Shanahan, On the effect of pH on spreading of surfactant solutions on hydrophobic surfaces, J. Colloid Interface Sci. 332 (2009) 497–504.
[21] J. Radulovic, K. Sefiane, M.E.R. Shanahan, Ageing of trisiloxane solutions, Chem. Eng. Sci. 65 (2010) 5251–5255.
[22] K.P. Ananthapadmanabhan, E.D. Goddard, P. Chandar, A study of the solution, interfacial and wetting properties of silicone surfactants, Colloids Surf. 44 (1990) 281–297.
[23] V. Starov, Static contact angle hysteresis on smooth, homogeneous solid substrates, Colloid Polym. Sci. 291 (2013) 261–270.
[24] R.E. Isele-Holder, B. Berkels, A.E. Ismail, Smoothing of contact lines in spreading droplets by trisiloxane surfactants and its relevance for superspreading, Soft Matter 11 (2015) 4527–4539.
[25] G. Karapetsas, R.V. Craster, O.K. Matar, On surfactant-enhanced spreading and superspreading of liquid drops on solid surfaces, J. Fluid Mech. 670 (2011) 5–37.
[26] P.E. Theodorakis, E.A. Muller, R.V. Craster, O.K. Matar, Superspreading: mechanisms and molecular design, Langmuir 31 (2015) 2304–2309.
[27] E. Ruckenstein, Effect of short-range interactions on spreading, J. Colloid Interface Sci. 179 (1996) 136–142.
[28] E. Ruckenstein, Superspreading: A possible mechanism, Colloids Surf. A Physicochem. Eng. Asp. 412 (2012) 36–37.
[29] P.E. Theodorakis, E.R. Smith, E.A. Müller, Spreading of aqueous droplets with common and superspreading surfactants, A molecular dynamics study, Colloids and Surfaces A: Physicochemical and Engineering Aspects 581 (2019).
[30] A.D. Nikolov, D.T. Wasan, A. Chengara, K. Koczo, G.A. Policello, I. Kolossvary, Superspreading driven by Marangoni flow, Adv. Colloid Interface Sci. 96 (2002) 325–338.
[31] S. Rafai, D. Sarker, V. Bergeron, J. Meunier, D. Bonn, Superspreading: aqueous surfactant drops spreading on hydrophobic surfaces, Langmuir 18 (2002) 10486–10488.
[32] H.-H. Wei, Marangoni-enhanced capillary wetting in surfactant-driven superspreading, J. Fluid Mech. 855 (2018) 181–209.
[33] N.M. Kovalchuk, O.K. Matar, R.V. Craster, R. Miller, V.M. Starov, The effect of adsorption kinetics on the rate of surfactant-enhanced spreading, Soft Matter 12 (2016) 1009–1013.
[34] N.M. Kovalchuk, J. Dunn, J. Dvies, M.J.H. Simmons, Superspreading on hydrophobic substrates: effect of glycerol additive, Colloids Interfaces 3 (2019).
[35] N.M. Kovalchuk, A. Trybala, V. Starov, O. Matar, N. Ivanova, Fluoro- vs hydrocarbon surfactants: why do they differ in wetting performance? Adv. Colloid Interface Sci. 210 (2014) 65–71.
[36] Z. Peng, C. Lu, M. Xu, Influence of substructures on the spreading ability and hydrolysis resistance of double-tail trisiloxane surfactants, J Surfact Deterg 13 (2010) 75–81.
[37] J. Lin, W. Wang, W.L. Bai, M.N. Zhu, C. Zheng, Z.L. Liu, X.F. Cai, D.D. Lu, Z.W. Qiao, F.Q. Chen, J.X. Chen, A gemini-type superspreader: synthesis, spreading behavior and superspreading mechanism, Chem. Eng. J. 315 (2017) 262–273.
[38] J. Shen, Y. Bai, X. Tai, W. Wang, G. Wang, Surface Activity, Spreading, and aggregation behavior of ecofriendly perfluoropolyether amide propyl betaine in aqueous solution, ACS Sustainable Chem Eng 6 (2018) 6183–6191.
[39] A. Czajka, C. Hill, J. Peach, J. Pegg, I. Grillo, F. Guittard, S.E. Rogers, M. Sagisaka, J. Eastoe, Trimethylsilyl Hedgehogs - A novel class of superefficient hydrocarbon surfactants, Phys. Chem. Chem. Phys. 19 (2017) 23869–23877.
[40] Surfactants: Chemistry, Interfacial Properties, Applications, Elsevier, Amsterdam, The Netherlands, 2001.
[41] N. Kumar, A. Couzis, C. Maldarelli, Measurement of the kinetic rate constants for the adsorption of superspreading trisiloxanes to an air/aqueous interface and the relevance of these measurements to the mechanism of superspreading, J. Colloid Interface Sci. 267 (2003) 272–285.
[42] Physical Properties of Glycerine and Its Solutions, Glycerine Producers' Association, New York, NY, USA, 1963.
[43] C.A. Schneider, W.S. Rasband, K.W. Eliceiri, NIH Image to ImageJ: 25 years of image analysis, Nat. Methods 9 (2012) 671–675.
[44] M. Sagisaka, D. Koike, Y. Mashimo, S. Yoda, Y. Takebayashi, T. Furuya, A. Yoshizawa, H. Sakai, M. Abe, K. Otake, Water/supercritical CO2 microemulsions with mixed surfactant systems, Langmuir 24 (2008) 10116–10122.
[45] D. Quere, Wetting and roughness, Annu. Rev. Mater. Res. 38 (2008) 71–99.